α-Cycloaltrin: Conformation and Properties in the Solid-State and Aqueous Solution

Stefan Immel, Guido E. Schmitt, and Frieder W. Lichtenthaler
Institute of Organic Chemistry, Darmstadt University of Technology, Germany

Introduction

The wealth of knowledge that has accumulated on the starch-derived cyclodextrins and their unique ability to form inclusion complexes[1] is contrasted by a peculiar paucity of data on cyclooligosaccharides composed of sugars other than glucose[2]. Except for certain cyclofructins, obtainable by bacterial action on the polysaccharide inulin[3], all of the non-glucose cyclooligosaccharides presently known have been acquired synthetically, requiring laborious multistep procedures. In this way, α(1→4)-linked cyclooligosaccharides composed of D-mannose[4] (i.e. α-, β- and γ-cyclomannin), of L-rhamnose[5] (α-cyclorhamnin), and of alternating D-mannose/L-rhamnose units[6] have been prepared, yet in so minute amounts as to preclude investigations into their inclusion complex behavior. Molecular modeling studies on α-cyclomannin[7] and its 6-deoxy-L-analog α-cyclorhamnin[2] showed their axially disposed 2-OH to point away from the cavity, thus fairly closely resembling α-cyclodextrin in backbone structure, cavity dimensions, and lipophilicity patterns.

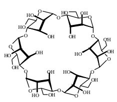

all-$^4C_1$ (**1a**)

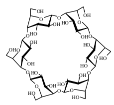

all-$^1C_4$ (**1b**)

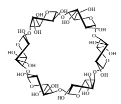

all-$^OS_2$ (**1c**)

The same, in fact, is to be expected for the cyclohexasaccharide with alternating D-mannose and L-rhamnose units. For α-cyclogalactin composed of six β(1→4)-linked galactopyranose residues, molecular modeling displayed an α-CD-like geometry, yet a distinctly different lipophilicity distribution such that the hydrophobic surface regions at the primary hydroxyl face are substantially enlarged.[7] More profound changes in shape, cavity dimensions, and guest binding properties are to be anticipated for cyclooligosaccharides with axially disposed 3-OH groups in the pyranoid rings - α-cycloallin for example - as these would be directed towards the cavity interior, resulting in considerable steric congestion that is likely to be released by deformation of the $^4C_1$ chairs. Topologically even more interesting is α-cycloaltrin, as the $^4C_1$ and $^1C_4$ conformations of α-altropyranoid chairs are very similar in stability[8] and, hence, in a macrocyclic array could elaborate various conformations, such as the *all*-$^4C_1$ (**1a**) or *all*-$^1C_4$ forms (**1b**), or in solution more likely, an equilibrium between the two, passing through the skew $^OS_2$-geometries (**1c**) of the pyranoid rings.

Solid State Structure

Most recently, the α-cycloaltrin (**1**) became available synthetically from the α-cyclodextrin by a straightforward four-step protocol[9] with 2,3-anhydro-α-cyclomannin as the key intermediate. The α-cycloaltrin (**1**) thus obtained, crystallized with alltogether 21 water molecules. Its X-ray structural analysis not only gave evidence of the water molecules built into the crystal lattice, but revealed the unique conformational features of the altropyranoid rings: neither the *all*-$^4C_1$ or the *all*-$^1C_4$ form are adopted; instead, there is a continuous succession of $^4C_1$ and $^1C_4$ altropyranoid chairs, entailing the macrocycle to be made up of three banana-shaped disaccharide portions of which one is depicted in conventional graphics:

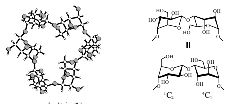

α-cycloaltrin (**1**)

The molecules have a compact, disk-shaped topology, being stacked in transposed layers rather than perpendicular above each other.

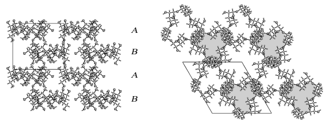

The extent to which the respective chair conformations are materialized is remarkable: nearly perfect geometry in the $^1C_4$ portions with six pyranoid ring torsion angles in the 52-58° range. The $^4C_1$ chairs, by contrast, are less impeccable, as one torsion angle (-47.7°) reveals some flattening at C-2 and C-3.

Another salient feature of the structure lies in the different orientation of the 6-OH groups: gauche-trans diposition in the three $^1C_4$ forms, in which the CH_2OH groups are directed towards the outside of the macrocycle, versus gauche-gauche arrangement in the three $^4C_1$ forms, their CH_2OH groups pointing towards the center of the macrocycle, therby closing it. Accordingly, the disk-shaped molecule has a shallow indentation on the one side, and a pronounced one, hole-like on the other.

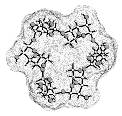

Ball and stick representation of the α-cycloaltrin (**1**) with the calculated[10] contact surface in dotted form.

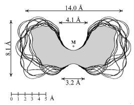

Cross section plot through the contact surface of **1** and approximate molecular dimensions (2-OH/3-OH side up).

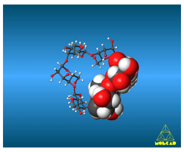

Ball-and-stick model representation of **1**, as generated by the MOLCAD program[11]. The macrocycle is thus made up of three banana-shaped disaccharide portions, of which one is presented in space filling form.

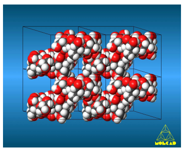

The α-cycloaltrin disks are stacked in transposed layers rather than perpendicular above each other; the empty space in between is occupied by water molecules, left off here for clarity.

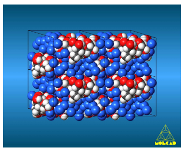

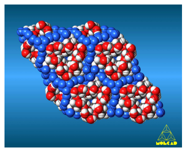

The molecules have a compact, disk-shaped topology, devoid of a cavity, and are embedded into a water matrix ($1 \cdot 21\ H_2O$).

NMR Analysis

In case this disk-shaped solid-state structure of α-cycloaltrin, already embedded in a water matrix is retained in aqeuous solution, not only separate sets of NMR signals are to be observed for the $^4C_1$ and the $^1C_4$ portions, but also distinctly different coupling patterns for the respective pyranoid ring protons as revealed by respective calculated *J*-values.

Table 1. Comparsion of the altropyranoid ring ^1H-^1H-coupling constants calculated for the $^4C_1$, $^1C_4$, and *all*-$^OS_2$ (skew) forms of the α-cycloaltrin with those found (800 MHz[12], D_2O, 30°C)

coupling constants [Hz][a]	$^4C_1$	$^1C_4$	$^OS_2$[b]	found	calc.[c]
$J_{1,2}$	2.2	8.0	4.0	4.73	4.9
$J_{2,3}$	2.7	10.2	10.2	8.19	8.3
$J_{3,4}$	3.4	2.4	4.5	3.71	3.5
$J_{4,5}$	9.7	1.4	6.4	5.32	5.5

[a] Calculation based on the Karplus-type H-C-C-H-torsion angle dependency of coupling constants, including the electronegativity effect of the substitution pattern by use of the generalized Haasnoot-equation[13]. [b] Data claculated of the HTA-derived global energy minimum *all*-skew form. [c] Least-squares fit for 26% $^4C_1$, 34% $^1C_4$, and 40% $^OS_2$.

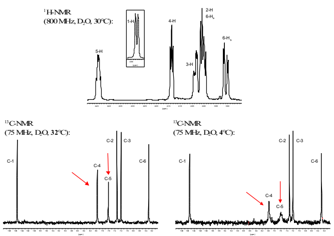

The $J_{2,3}$ of 8.2 Hz at 30°C in D_2O decreases to 7.6 and 7.1 Hz at 20 and 4°C, respectively; more profound effects are observed for the C-4 and C-5 signals, which are sharp singlets at 30°C, yet show substantial broadening at 4°C. Accordingly, α-cycloaltrin in water does not adopt a fixed geometry, as e.g. the *all*-$^OS_2$-form; rather, the D-altropyranoid rings, tied up in a macrocyclic "strait-jacket", adopt a variety of conformations within the $^4C_1 \leftrightharpoons {}^OS_2 \leftrightharpoons {}^1C_4$ pseudorotational itinerary, and this necessarily in a coordinated way: flexure of one altropyranoid chair into the intermediate skew $^OS_2$-form - via the respective half-chair transition states - entails the two adjoining altrose chairs to follow suit, thereby eliciting a consecutive "rolling around" in the conceivably elliptically distorted macrocycle.

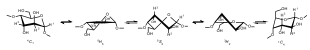

NMR data provide an averaged picture thereof, and - through the comparatively large $J_{1,2}$ and, particularly, $J_{2,3}$ couplings - give evidence that the position of the equilibrium lies pronouncedly on the $^1C_4 \leftrightharpoons {}^OS_2$ side.

Molecular Modeling

In contrast to the solid-state structure of α-cycloaltrin (**1**), the *all*-skew $^OS_2$-geometry **1c**, which in fact emerges from HTA-calculations[14] as the global energy minimum structure, which features a through-going cavity and a pyranose tilt inverse to that of the cyclodextrins.

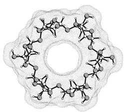

Contact surface of the *all*-skew $^OS_2$-form **1c** (emerges from HTA calculations) with a ball-and-stick model insert.

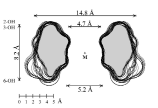

Cross section plot of a plane perpendicular to the macrocycle main plane with the contact surface of the α-cycloaltrin **1c**.

Whether, however, the *all*-skew form **1c** is adopted in aqueous solution - HTA simulations are against vacuum boundaries rather than a solvation shell - remains open. If prevalent in aqueous solution, its cavity is conceivably filled with water thus not only the six primary, but the 12 secondary hydroxyl groups are likely to satisfy their hydrogen bonding requirements towards the solvent rather than intramolecularly. This results in a tightly associated first water shell around **1** which will have to follow any geometry changes within the macrocycle. This hydration sphere could readily be characterized by molecular dynamics simulations (MD) in water, yet had no relevance to unraveling the nature of the $^4C_1 \leftrightharpoons {}^1C_4$ scrambling observed in the NMR, since not only the solid-state $^4C_1/^1C_4$-structure of **1**, when subjected to a 600 picosec MD simulation in a box of water, remained in that geometry, but the *all*-skew $^OS_2$ form did so too. Accordingly, no appreciable flexure or flip over of the pyranoid chairs or skew forms to alternate topologies takes place within a 600 picosec time frame of unconstrained MD simulations, i.e. profound conformational changes within the macrocycle are comparatively slow, obviously requiring the millisec time frame of NMR resolvability to occur.

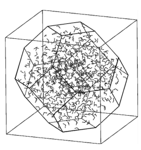

Snapshot of a MD simulation of α-cycloaltrin **1** surrounded by 606 water molecules (boxsize of the truncated octahedron 32 Å).

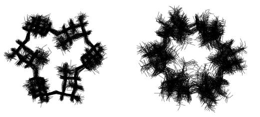

Superimposition of 60 α-cycloaltrin (solid-state structure left, *all*-skew-form right) snapshot geometries taken in 10 ps intervals from 600 ps molecular dynamic simulations on an assembly comprising α-cycloaltrin in a box of 606 and 611 water molecules, respectively.

References

[1] (a) J. Szejtli, *Cyclodextrins and Their Inclusion Complexes*, Académiai Kiadó, Budapest **1982**. (b) D. Duchêne (Ed.), *Trends in Cyclodextrins and Derivatives*, Edit. de la Santé, Paris **1991**. (c) G. Wenz, *Angew. Chem.* **1994**, *106*, 851-870. *Angew. Chem. Int. Ed. Engl.* **1994**, *33*, 803-822. (d) J. Szejtli, L. Szente (Eds.), *Proceedings of the 8th International Symposium on Cyclodextrins*, Kluwer Acad. Publ., Dordrecht, **1996**, 600pp.

[2] For a recent review, see: F.W. Lichtenthaler, S. Immel, *J. Inclusion Phenom. Mol. Recognit. Chem.* **1996**, *25*, 3-16.

[3] (a) M. Kawamura, T. Uchiyama, T. Kuramoto, Y. Tamura, K. Mizutani, *Carbohydr. Res.* **1989**, *192*, 83-90. (b) M. Sawada, T. Tanaka, Y. Takai, T. Hanafusa, T. Taniguchi, M. Kawamura, T. Uchiyama, *ibid.* **1991**, *217*, 7-17.

[4] M. Mori, Y. Ito, T. Ogawa, *Carbohydr. Res.* **1989**, *192*, 131-146; M. Mori, Y. Ito, J. Izawa, T. Ogawa, *Tetrahedron Lett.* **1990**, *31*, 3191-3194.

[5] M. Nishizawa, H. Imagawa, Y. Kan, H. Yamada, *Tetrahedron Lett.* **1991**, *32*, 5551-5554; *Chem*. Pharm. *Bull.* **1994**, *42*, 1356-1365.

[6] P.R. Ashton, C.L. Brown, S. Menzer, S.A. Nepogodiev, J.F. Stoddart, D.J. Williams, *Chem. Eur. J.* **1996**, *2*, 580-591.

[7] F.W. Lichtenthaler, S. Immel, *Tetrahedron: Asymmetry* **1994**, *5*, 2045-2060.

[8] (a) S.J. Angyal, *Aust. J. Chem.* **1968**, *21*, 2737-2746. (b) S.J. Angyal, V.A. Pickles, *ibid.* **1972**, *25*, 1695-1710.

[9] Y. Nogami, K. Fujita, K. Ohta, K. Nasu, H. Shimada, C. Shinohara, T. Koga, (J. Szejtli, L. Szente, Eds.), *Proceedings 8th Internat. Symp. on Cyclodextrins*, Kluwer Acad. Publ. Dordrecht, **1996**, pp. 99-102.

[10] (a) B. Lee, F.M. Richards, *J.Mol. Biol.* **1971**, *55*, 379-400. (b) M.L. Connolly, *J. Appl. Cryst.* **1983**, *16*, 548-558; *Science* **1983**, *221*, 709-713.

[11] (a) J. Brickmann, *MOLCAD - MOLecular Computer Aided Design*, Darmstadt University of Technology, **1997**. (b) J. Brickmann, *J. Chim. Phys.* **1992**, *89*, 1709-1721.

[12] We are most grateful to Prof. Dr. C. Griesinger and Dr. H. Schwalbe, Institut für Organische Chemie, Universität Frankfurt/Main, for kindly determining the ^{1}H and ^{13}C NMR data of **1** at 800 and 200 MHz, respectively.

[13] (a) M. Karplus, *J. Chem. Phys.* **1959**, *30*, 11-15. (b) C.A.G. Haasnoot, F.A.A.M. De Leeuw, C. Altona, *Tetrahedron* **1980**, *36*, 2783-2792.

[14] High Temperature Annealing (HTA) calculations were performed with a force field program specially adapted to carbohydrates, comprising application of the verlet integrator in the MD simulation program CHARMM with a timestep of 1fs at constant temperature and dielectric constant ε = 1. Out of MD trajectories at 1200K (4059 ps) every 1000fs the respective conformation was allowed to cool down to 300K with a rate of 10 K/fs, was held there for additional 1100 fs, and was subsequently fully energy-minimized by an adapted Newton-Raphson algorithm of the CHARMM22 program package.